Use of Midlatitude Soil Moisture and Meteorological Observations to Validate Soil Moisture Simulations with Biosphere and Bucket Models

ALAN ROBOCK, KONSTANTIN YA. VINNIKOV, AND C. ADAM SCHLOSSER

Department of Meteorology, University of Maryland, College Park, Maryland

NINA A. SPERANSKAYA

State Hydrological Institute, St. Petersburg, Russia

YONGKANG XUE*

Department of Meteorology, University of Maryland, College Park, Maryland

(Manuscript received 12 February 1993, in final form 18 April 1994)

ABSTRACT

Soil moisture observations in sites with natural vegetation were made for several decades in the former Soviet Union at hundreds of stations. In this paper, the authors use data from six of these stations from different climatic regimes, along with ancillary meteorological and actinometric data, to demonstrate a method to validate soil moisture simulations with biosphere and bucket models. Some early and current general circulation models (GCMs) use bucket models for soil hydrology calculations. More recently, the Simple Biosphere Model (SiB) was developed to incorporate the effects of vegetation on fluxes of moisture, momentum, and energy at the earth's surface into soil hydrology models. Until now, the bucket and SiB have been verified by comparison with actual soil moisture data only on a limited basis. In this study, a Simplified SiB (SSiB) soil hydrology model and a 15-cm bucket model are forced by observed meteorological and actinometric data every 3 h for 6-yr simulations at the six stations. The model calculations of soil moisture are compared to observations of soil moisture, literally "ground truth," snow cover, surface albedo, and net radiation, and with each other.

For three of the stations, the SSiB and 15-cm bucket models produce good simulations of seasonal cycles and interannual variations of soil moisture. For the other three stations, there are large errors in the simulations by both models. Inconsistencies in specification of field capacity may be partly responsible. There is no evidence that the SSiB simulations are superior in simulating soil moisture variations. In fact, the models are quite similar since SSiB implicitly has a bucket embedded in it. One of the main differences between the models is in the treatment of runoff due to melting snow in the spring—SSiB incorrectly puts all the snowmelt into runoff. While producing similar soil moisture simulations, the models produce very different surface latent and sensible heat fluxes, which would have large effects on GCM simulations.

1. Introduction

Soil moisture is one of the most important components of the climate system. Crucial questions about the future climate predicted for a world made warmer by enhanced greenhouse gases, such as summer drying of midcontinent agricultural regions, depend on detailed knowledge of the interactions of soil moisture with the climate. Climate models, however, use primitive parameterizations and have inadequate data with which to improve the parameterizations or to compare to simulations (Gleick 1989). The summer drying phenomenon (e.g., Manabe et al. 1981; Wilson and Mitchell 1987), for example, is a combination of the processes involving soil moisture, precipitation, time of snowmelt in the spring, partitioning of snowmelt into the soil or runoff, water table variations, and potential evaporation due to warmer temperatures. To determine whether midcontinental drying is a robust prediction, soil moisture must be properly simulated.

Soil moisture anomalies serve the same function for land that sea surface temperature anomalies serve for the ocean, providing a storage and forcing that is longer than the timescale of the atmosphere. Delworth and Manabe (1988, 1989) have shown how soil moisture interactions can produce redder spectra of many meteorological and hydrological variables in a GCM simulation. These simulations were done with a simple

* Current affiliation: Center for Ocean–Land–Atmosphere Studies, Calverton, Maryland.

Corresponding author address: Dr. Alan Robock, Department of Meteorology, University of Maryland, College Park, MD 20742-2425.
E-mail: alan@atmos.umd.edu

TABLE 1. Heat-balance stations.

Station	Latitude (°N)	Longitude (°E)	Soil type/water table depth Observed hydrological properties (cm) Total water-holding capacity (W_0)	Field capacity (W_f)	Wilting level (W_*)
Khabarovsk, Russia	48.5	135.2	brown earth podzolic, gleic, heavy loamy/very deep		
top 50 cm			26.2	14.1	5.5
top 1 m			48.3	23.0	14.1
Kostroma, Russia	57.8	41.0	black earth leached, loamy/~18 m		
top 50 cm			—	—	1.2
top 1 m			—	—	2.7
Ogurtsovo, Russia	54.9	83.0	dark chestnut, heavy loamy/7–8 m		
top 50 cm			28.6	11.5	4.7
top 1 m			55.7	20.1	8.2
Tulun, Russia	54.6	100.6	derno-wooded carbonic leached, heavy loamy/>20 m		
top 50 cm			30.2	—	6.1
top 1 m			54.8	—	13.7
Uralsk, Kazakhstan	51.3	51.4	dark chestnut, heavy loamy/7–8 m		
top 50 cm			27.1	10.1	5.5
top 1 m			48.3	17.0	13.0
Yershov, Russia	51.4	48.3	dark chestnut, clayey/30–35 m		
top 50 cm			25.6	10.8	7.7
top 1 m			46.4	19.9	15.9

— Missing

15-cm bucket model of soil moisture—the model used at the Geophysical Fluid Dynamics Laboratory (GFDL) and the National Center for Atmospheric Research (NCAR). The Goddard Institute for Space Studies (GISS) uses a slightly more complex model involving two soil layers (Hansen et al. 1983), while the U.K. Meteorological Office has experimented with different runoff schemes (Mitchell 1983).

In the past decade, more complex land parameterization schemes that incorporate biophysical control of evaporation have been developed [e.g., the Biosphere–Atmosphere Transfer Scheme (BATS)—Dickinson et al. (1986); the Simple Biosphere (SiB) model—Sellers et al. (1986); Xue et al. (1991)]. These schemes are now beginning to be used in long-term climate simulations, and verification of their accuracy is crucial. SiB has not been used in a climate model for $2 \times CO_2$ calculations yet, but simulations of the current climate (Sato et al. 1989) and simulations of Amazon deforestation (Shukla et al. 1990; Nobre et al. 1991) show large effects of the biophysical control of evaporation. Although SiB has been tested with data from the Tropics (Sellers and Dorman 1987; Sellers et al. 1989), soil moisture data for higher latitudes have not until now been used to verify the model (Dorman and Sellers 1989; Sato et al. 1989). Only synthetic, model-based datasets have been available, such as the Palmer Drought Index (Palmer 1968) and calculations by Mintz and Serafini (1992) and Schemm et al. (1992).

The main goal of this paper is to develop a method and give an example of how routine meteorological observations and measurements of soil moisture can be used for testing and intercomparison of different land surface water and energy balance models. The work reported in this paper may be considered a pilot study, addressing the issues of comparing observations with output from two very different land surface schemes. Its results may have relevance to the Project for Intercomparison of Land-Surface Parameterization Schemes (PILPS) (Henderson-Sellers et al. 1993).

Atmospheric GCMs are affected by vertical fluxes of latent heat, sensible heat, and radiation from the land surfaces, not directly by soil moisture. But soil moisture, snow depth, runoff, and water table depth have important impacts on hydrology and agriculture. In this experiment we can directly evaluate the shortwave radiation, net longwave radiation, soil moisture, and snow depth outputs of the models, but we do not have data for these stations to directly evaluate the complete water and energy budgets. However, we are currently conducting similar experiments for a water balance station at Valdai, Russia, that includes all these quantities in three different catchments, and this will be the subject of another paper.

To investigate the question of whether a simple bucket model or a complex biosphere model can accurately calculate soil moisture, radiation, and snow depth, we use actual meteorological and actinometric data observed every 3 h for a 6-yr period (1978–1983) for six stations distributed across the former Soviet Union (Table 1, Fig. 1) to force a standard bucket model (identical to that used at GFDL and NCAR) and the Simplified SiB (SSiB) version (Xue et al. 1991)

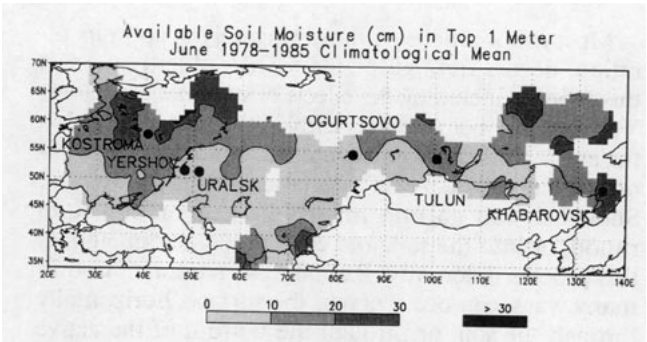

FIG. 1. Locations of six stations used for simulations (see Table 1) superimposed on a map of June mean available soil moisture for the period 1978–1985 from the 130-station dataset.

of SiB. We compare the resulting simulations of soil moisture with actual observations taken at these six stations, literally ground truth. The soil moisture observations were taken with the thermostat-weight (gravimetric) technique every 10 days during the growing season and once a month when the ground was frozen, and are described in detail below.

We recognize that both the bucket and biosphere models have shortcomings, but we decided to use versions identical to those used for past and recent GCM experiments so we can evaluate how well these versions agree with observations. All six sites have a natural grass cover, and so we used SSiB vegetation type 7, grass cover, for all calculations.

Because the observations we use both to drive the models and to evaluate their outputs were taken at a specific station, and the models represent the physics at a specific point, there is no problem with scale matching in our experiments. Whether these schemes can be used with GCM gridbox-size forcing and reproduce the same scale physics cannot be addressed in this study except to say that the observations are from regions specifically chosen to be representative of large areas.

We first present a general discussion of soil moisture, defining terms and describing measurement methods. Next we describe the specific dataset that we used and the soil moisture models. Then our experiments with the standard models are presented. Finally, we discuss the results and give conclusions.

2. Soil moisture

a. Background

Both soil parameterizations used in this study, the bucket and SSiB, incorporate a simplistic view of soil hydrology, as detailed here. More sophisticated treatments of water in soil have been incorporated into soil water calculations (Abramopoulos et al. 1988; Henderson-Sellers et al. 1993), but our data do not allow evaluation of the value of such complex schemes in GCM soil hydrology parameterizations. This is because these complex treatments require knowledge of a large number of parameters that are not generally available anywhere in the world, including Russia.

Consider the topmost 1 m of soil (Fig. 2). An analysis of the contents of this layer would find varying amounts of soil, water, air, and biological material, depending on the soil properties (texture, composition, and density), vegetation, soil wetness, and topography. Approximately one-half of the volume contains soil and biomass. If the remaining fraction (the porosity) were completely full of water, the soil would contain its *total water-holding capacity*, W_0, and the water table would be at the surface. The SSiB grass cover type has a porosity of 0.42. Therefore, for any layer, $W_0 = PD$, where P = porosity and D = depth (thickness) of layer. In SSiB, for grass cover, the soil is divided into layers of 2-, 47-, and 100-cm thickness (Fig 3), and this discussion applies to each of these layers. Other types of vegetation would have different values of some of these parameters.

To understand the various water reservoirs in soil, it is sometimes useful to think of the following simplistic partitioning, as shown in Fig. 2: of all the water in the top 1 m, approximately one-third can be lost to gravity, one-third is unavailable—locked in the pores of the soil—and one-third can be lost to evapotranspiration (Y. Sud 1992, personal communication). When the water table is between the surface and 3 m, some of the water lost to gravity will be balanced by upward capillary motion (Vinnikov and Yeserkepova 1991), but this is not relevant for any of the stations used here, as the water table depth is greater than or equal to 4 m for all stations (Table 1).

The amount of plant-unavailable water determines the *wilting level* W_*, because plants wilt when the soil moisture reaches this level. This water can be removed

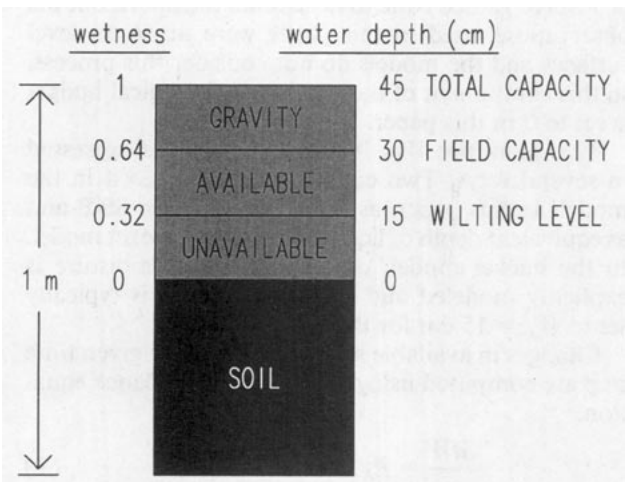

FIG. 2. Illustration of the typical contents of the top 1 m of soil, with the three water partitions. On the left are typical values of soil wetness from SSiB, and on the right, typical values of water depth from the bucket model.

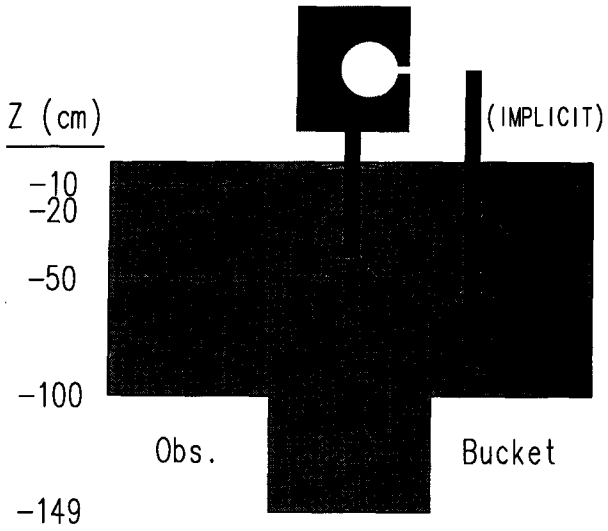

FIG. 3. Vertical resolution of soil moisture observations and the SSiB and bucket models. For grass, SSiB explicitly includes vegetation with stomatal resistance and roots in the top two model layers and 1% of the third layer. The bucket implicitly includes vegetation that can extract moisture from the entire 1-m bucket.

from the soil by putting the soil in an oven and heating it. The remaining portion of soil moisture is the amount that can be extracted by evapotranspiration. This portion is called the plant-available moisture W. The *field capacity* W_f is the maximum amount of W that soil can sustain against gravity: W_0, W_*, and W_f all depend on soil and vegetation types. SSiB distinguishes in its calculations between evaporation from the soil surface and transpiration through vegetation. The wilting level, therefore, is slightly less than what cannot be extracted by plants since some additional amount can be extracted by surface soil evaporation.

If the soil has complex topography, water can also be lost (or gained) due to horizontal transport, but the observations used in this paper were made on level surfaces and the models do not consider this process, so this component of the soil and hydrological budget is set to 0 in this paper.

The quantities W_0, W_*, and W_f can be expressed in several ways. Two common ways are used in the models in this paper: as a percent of W_0 in SSiB and as equivalent depth of liquid water in the bucket model. In the bucket model, only the available moisture is explicitly modeled and the field capacity is typically set to $W_f = 15$ cm for the top 1 m of soil.

Changes in available soil moisture over a given time step are computed using a simple water balance equation:

$$\frac{dW}{dt} = P_R - E + M - R, \qquad (1)$$

where W is available soil moisture, P_R is rainfall, E is evapotranspiration, M is snowmelt, R is runoff, and t is time.

Most evaporation, or more precisely evapotranspiration, occurs through plants. SSiB explicitly models this process, including the effects of stomatal resistance. Vegetation is included implicitly in the bucket model—the entire top 1 m of soil could not contribute to evaporation in the bucket if vegetation were not present. Snowmelt can go into immediate evaporation, into runoff, or into the soil, and each model parameterizes this process differently. Runoff, also parameterized in many ways, can occur across the surface, horizontally through the soil, or through the bottom of the active soil layer. Runoff, as measured in streams and rivers, actually has a time lag, but results here for both models are presented as the instantaneous amount. River routing models (e.g., Miller and Russell 1992) can be used to actually determine the fate of the runoff. Dooge (1992) gives a detailed discussion of the small-scale aspects of runoff modeling.

b. Observations

Vinnikov and Yeserkepova (1991) discuss in detail the Russian data used in this paper, and they are described briefly here. This was one of the first attempts to use these soil moisture measurements for testing climate model results. [We use the term "Russia" here for convenience, even though one of the stations used in this paper (Uralsk) is just across the border in Kazakhstan and all were in the Soviet Union when the observations were made.]

This analysis is possible because in the 1930s the Hydrometeorological Service of the Soviet Union organized a unified system of soil moisture measurements, using the existing network of meteorological and agrometeorological stations and opening new stations. At some of the more than 3000 Soviet agrometeorological and water balance stations, an additional program of measurement of soil moisture was started in 1967 at more than 200 permanent sites with natural, mostly meadow, vegetation.

Figure 1 shows the June average available soil moisture for the period 1978–1985 in the top 1 m of soil for 130 of these stations for which we have data, and the locations of the six stations (Table 1) we have chosen, based on their high data quality and geographical distribution, for our experiments. At each of these stations, soil moisture measurements and meteorological data are observed at a plot planted with grass. Thus, the same type of natural vegetation is used at all plots, irrespective of the surrounding vegetation, which could be grass, forest, agricultural fields, or other types. Our preliminary analysis of data from the Valdai water balance research station shows that soil moisture is almost the same in grass-covered and forest plots, although other hydrological variables, such as runoff and water table, are not.

The choice of plots at each station was made to satisfy the following conditions. 1) The plot is a flat piece

of land with an area greater than or equal to 0.10 ha. 2) The soil type is representative of the main soil type and landscape of the region and does not differ significantly from the prevailing soil type and landscape of the climatic zone. 3) The mean depth of the water table and its seasonal variations are typical for a large area. The temporal resolution of the measurements is 10 days in the warm season and one month during the winter. Reference books that we used contain soil moisture data for layers 0–10, 0–20, 0–50, 0–100, and sometimes, 0–150 cm. Data for Tulun and Ogurtsovo come from publications of the West-Siberia Territorial Hydrometeorological Administration in Novosibirsk. For Yershov and Kostroma, data come from the Upper Volga Territorial Hydrometeorological Administration in Gorky. Uralsk data are from the Alma-Ata Hydrometeorological Observatory in Alma-Ata, and Khabarovsk data are from the Far East Territorial Hydrometeorological Administration in Khabarovsk.

The method of soil moisture observation is based on extraction of soil core samples and use of a thermostat-weight technique for soil water content measurements. Cores of soil are extracted from at least four different points at each plot in 10-cm segments. A sample from each 10-cm segment is then weighed, oven dried, and weighed again. The difference in mass gives the total soil moisture in the sample. The plant-unavailable portion (wilting level), previously determined from agricultural experiments at that station with an oat crop [see Vinnikov and Yeserkepova (1991) for details], is then subtracted from this total, leaving the available soil moisture, expressed as depth of liquid water. Special measurements of agrophysical constants of soil for each plot for each 10-cm layer at each station determine field capacity, total water-holding capacity, and wilting coefficient, and are shown in Table 1 for our stations with 50-cm resolution.

c. *Error analysis*

To compare model results to observations, it is useful to have an idea of the uncertainty of the observed values. The root-mean-square error of the soil moisture measurements can be obtained by using the statistical method proposed by Gandin (1965), which is based on extrapolation of empirical estimates of the spatial (or temporal) autocorrelation function to distance (or time) lag equal to zero. Vinnikov and Yeserkepova (1991), following the theoretical conclusions of Delworth and Manabe (1988), showed that empirical estimates of temporal autocorrelation functions of soil moisture for the upper 1 m can be successfully approximated as the sum of the white and red noises:

$$r(t) = \begin{cases} 1 + a & \text{for} \quad t = 0 \\ e^{-(t/T)} & \text{for} \quad t \neq 0, \end{cases}$$

where r is the autocorrelation function and T is the autocorrelation timescale. Parameter a characterizes the part of the variance due to uncorrelated random processes and can be ascribed to random errors of measurement.

To illustrate the calculation of error, an empirical estimate of the temporal autocorrelation function of 1-m layer soil moisture for the station Uralsk is plotted in Fig. 4 by circles connected with thin lines, using data for 1968–1985. The thick straight line in the figure is our best fit of $r(t)$ to these data and corresponds to an approximation of $r(t)$ with $T = 1.9$ months and $a = 0.1$. The estimated standard deviation (s) of soil moisture for this station is 2.3 cm. The rms error of soil moisture measurements is equal to $s[a/(1 + a)]^{1/2} = 0.7$ cm. Analogous estimates presented by Vinnikov and Yeserkepova (1991) for several other stations show that empirical estimates of the a parameter usually do not exceed the value of 0.1 and that the root-mean-square error of soil moisture in the upper 1-m layer measurements does not exceed the value of 1 cm. Of course, errors can vary significantly from season to season and from station to station. But we can see from this analysis that random errors of observations will not influence the comparisons with model simulations made later in the paper.

3. Forcing and verification data

The models (described in the next section) were initialized with observed values of soil moisture and snow cover, and then run for the 6-yr timespan of data

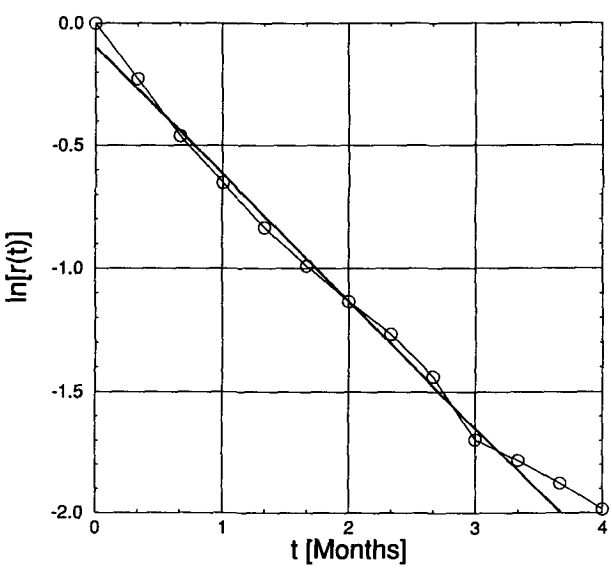

FIG. 4. Estimated autocorrelation function of 1-m soil moisture for Uralsk, using data for 1968–1985 (circles connected with thin lines), and the best fit of the theoretical autocorrelation function (thick straight line). The intercept of the thick line with the ordinate at $t = 0$ gives the estimate of the parameter a (= 0.1).

(1978–1983) with a time interval of 3 h. For the bucket model, consistent with the standard NCAR and GFDL schemes, running-mean diurnal averages of all the forcing parameters (with the exception of precipitation) were taken. However, for the SSiB experiments, we used 3-h time resolution of the forcing parameters, and thus diurnal variations were maintained. These forcing parameters were then used to force the model directly or to supply values to algorithmic arguments used within the models.

For each of the stations, runs of both models were performed using the following meteorological and actinometric data as forcing at 3-h intervals:

1) Q, total incoming shortwave radiation (W m^{-2})
2) T_a, air temperature at standard level of measurement (°C)
3) T_d, dewpoint temperature at standard level of measurement (°C)
4) P, precipitation (mm) = P_R (rainfall, when $T_a > 0$°C) + P_S (snowfall, when $T_a \leq 0$°C)
5) c_L, lower cloud cover fraction
6) c_T, total cloud cover fraction
7) $|V|$, wind speed at standard level of measurement (m s^{-1})
8) p_a, air pressure at standard level of measurement (mb).

Variations of the last variable play a negligible role in the calculations, and one could substitute the climatological value for each station without changing the results.

Observations of meteorological data for the period 1978–1983 are the regular measurements taken eight times per day (0000, 0300, 0600, 0900, 1200, 1500, 1800, and 2100) at the same time for all the territory of the former Soviet Union (Moscow legal time, Greenwich time plus 3 h). We obtained these data on magnetic tapes from the World Data Center B in Obninsk.

The actinometric data come from the regular measurements of the Russian actinometric station network. Incoming solar radiation and surface albedo were measured with pyranometers, and net total radiation was measured with net radiometers. These measurements are taken six times per day (0030, 0630, 0930, 1230, 1530, and 1830) at the mean local solar time. They were digitized on magnetic tapes and quality controlled in St. Petersburg at the Main Geophysical Observatory.

For individual instances of missing data (meteorological and actinometric), we did a linear interpolation using the time steps immediately before and after the missing time step to replace the missing value. The shortwave radiation data for Ogurtsovo for August 1979 were missing, and we replaced them with a linear regression with respect to total cloud cover using the remaining Augusts' data.

Although it would be possible to force the models with the observed net radiation, this would require that the upward longwave radiation be independent of surface temperature. We calculate, rather than specify, upward longwave radiation and use a parameterization for downward longwave radiation in order to allow the surface temperature to be a free variable and be calculated. This also allows us to use the net radiation to verify the calculations.

4. Hydrology models

This section gives a general description of the land surface hydrology models used for this study: a relatively simple bucket hydrology model with no explicit vegetation canopy, and a more sophisticated biosphere model that includes a canopy layer with a stomatal resistance parameterization and multiple, interactive subsurface soil layers, illustrated in Fig. 3.

a. Bucket model

The bucket model constructed for this study is identical to current GCM versions [Manabe 1969 (GFDL); Williamson et al. 1987 (NCAR CCM1)]. The model assumes a 15-cm field capacity of available soil moisture in the uppermost 1 m of soil. Changes in available soil moisture over a given time step are computed using the water balance equation [(1)].

In the original bucket model formulation (Budyko 1956), a provision was made for a portion of precipitation to run off immediately. In current GCMs, however, the choice was made to not allow any runoff when the bucket was not full (Manabe 1969; Williamson et al. 1987), and we have chosen this GCM assumption of bucket runoff.

Snowmelt is calculated in a manner identical to the standard GFDL GCM and NCAR CCM buckets (Manabe 1969; Williamson et al. 1987). Precipitation that falls when the air temperature is at or below freezing is assumed to be snowfall and is allowed to immediately accumulate on the ground. With a snow-covered surface, no changes of soil moisture are allowed through evaporation and precipitation. Rather, sublimation and precipitation (in the form of snowfall) change the snow depth. However, if surface temperature (T_s) is diagnosed as above freezing from the surface energy balance (described later), the snowmelt (calculated by setting T_s = 273.16 K and using the excess energy from the surface energy budget to melt the snow) is allowed to enter the soil and increase soil moisture. All of the snowmelt is allowed into the soil when the bucket is not full.

The soil is allowed to evaporate at its potential rate until it reaches a critical value of soil moisture, W_C, assumed to be 75% of its field capacity. For soil moisture values lower than W_C, evaporation is then given as a fraction of its potential rate:

$$E = \beta E_p(T_s), \tag{2}$$

where

$$\beta = \begin{cases} 1 & \text{for } W \geq W_C \\ \dfrac{W}{W_C} & \text{for } W < W_C, \end{cases}$$

$W_C = 0.75 W_f$,
$E_p(T_s)$: potential evaporation, and
T_s: surface temperature.

The parameterization of potential evaporation is prescribed following that of Budyko (1956). Potential evaporation is given by a bulk aerodynamic relation,

$$E_p(T_s) = C_D \rho |V| [q_s(T_s) - q_a], \tag{3}$$

where C_D is the bulk transfer coefficient = 0.003, ρ is the density of air at the standard level of measurement, $|V|$ is the wind speed at the standard level of measurement, $q_s(T_s)$ is the specific humidity of saturated air at surface temperature T_s, and q_a is the specific humidity of air at the standard level of measurement. The value of C_D is the same as used in the GFDL GCM for all land surfaces (R. Wetherald 1992, personal communication).

Milly (1992) recently noted that within GCM bucket hydrology schemes, actual surface temperatures are used to compute potential evaporation rates, which is inconsistent with the theory upon which the parameterizations are based (Budyko 1956). To achieve a consistent parameterization, a saturated (hypothetically) surface temperature must be used in the calculation of potential evaporation. However, for our control case, actual surface temperatures were used to calculate potential evaporation in order to simulate the standard GFDL and NCAR CCM GCM bucket models.

The surface temperature calculation is determined by a basic energy balance requirement. By assuming the thermal inertia of the soil to be 0 and soil longwave emissivity equal to be 1, the surface energy balance becomes

$$Q(1 - \alpha) + L_D - \sigma T_s^4 - LE - H = 0, \tag{4}$$

where Q is total incoming shortwave radiation, α is surface albedo, L_D is downward longwave radiation, σT_s^4 is upward longwave radiation from surface, σ is the Stefan–Boltzman constant = 5.67×10^{-8} W $(m^2\ K^4)^{-1}$, L is latent heat of vaporization = 2.50×10^6 J kg^{-1}, E is evapotranspiration, and H is sensible heat flux.

The energy balance approach in (4) is appropriate for a land surface with no diurnal cycle since the thermal inertia and/or subsurface heat flux terms that should normally appear on the rhs of the equation would be small. Use of the bucket model for a diurnal cycle calculation would require these terms.

Although measured values of albedo were contained within the forcing dataset, the bucket model contains a scheme to calculate albedos. We therefore calculated the albedo and used the observations to validate the model. The parameterization is identical to the GFDL scheme (Manabe 1969), which prescribes a base albedo value for various vegetation surfaces and modifies albedo during snow cover conditions according to surface temperature and snow cover thickness.

For grass cover without snow cover,

$$\alpha = \alpha_{\text{base}} = 0.18. \tag{5}$$

This value corresponds almost exactly to the observations from all the stations of albedo of the natural grass cover when not covered by snow.

For grass cover with thick snow cover (≥2.0-cm water equivalent depth),

$$\alpha = \alpha_{\text{snow}}, \tag{6}$$

where

$$\alpha_{\text{snow}} = 0.60 \quad (\text{if } T_s \leq T_{\text{crit}} = -10°\text{C})$$

$$\alpha_{\text{snow}} = 0.45 \quad (\text{if } T_s = T_{\text{fra}} = 0°\text{C})$$

$$\alpha_{\text{snow}} = \frac{0.45(T_{\text{fra}} - T_s) + 0.60(T_s - T_{\text{crit}})}{T_{\text{fra}} - T_{\text{crit}}}$$

$$(\text{if } T_{\text{crit}} < T_s < T_{\text{fra}}).$$

For grass cover with thin snow cover (<2.0-cm water equivalent depth),

$$\alpha = \alpha_{\text{base}} + (0.5 D_S)^{1/2}(\alpha_{\text{snow}} - \alpha_{\text{base}}), \tag{7}$$

where D_S is the water equivalent snow cover depth (cm).

Downward longwave radiation measurements were not supplied by the actinometric dataset and, as a result, had to be calculated. Sellers et al. (1989) suggested that the simple bulk Monteith (1961) formula is suitable for use within SiB model calculations, but the Satterlund (1979) scheme provides improved estimates for the apparent clear-sky emissivity of atmosphere ϵ_a especially when temperatures are below 0°C, so we used it to calculate ϵ_a and the Monteith formulation for the effects of clouds:

$$L_D = \epsilon_a(1 + nc^2)\sigma T_a^4, \tag{8a}$$

where ϵ_a is $1 - \exp(-e_a^{T_a/b})$ = apparent clear-sky emissivity of atmosphere, n is 0.2 for low cloud types or 0.04 for cirrus cloud types, c is cloud cover fraction, T_a is air temperature at the standard level of measurement, e_a is vapor pressure at the standard level of measurement (mb), and b is the empirical constant = 2016 K. Monteith (1961), however, defines "low cloud" as stratus, cumulus, altostratus, and altocumulus, the last two of which are conventionally classified as "middle cloud types." Since our dataset provides only lower cloud fraction (c_L) (which uses the conventional

meaning of stratus, nimbostratus, and cumulus) and total clouds (c_T), we modified (8a) to partition the parameter n to the appropriate cloud types. Using data from Hahn et al. (1984), we determined that over Russia when clouds were present, but there were no low clouds, approximately 50% of the time there were middle clouds and approximately 50% of the time there were high clouds. Therefore, the fractions of middle clouds c_M and high clouds c_H are the same and equal to $0.5(c_T - c_L)$. The equation for L_D then becomes

$$L_D = \epsilon_a(1 + 0.2(c_L + c_M)^2 + 0.04c_H^2)\sigma T_a^4. \quad (8b)$$

Sensible heat flux is calculated using a bulk relation analogous to potential evaporation (Williamson et al. 1987),

$$H = C_p^* \rho C_D |V|(T_s - T_a), \quad (9)$$

where C_p^* = specific heat of moist air.

The surface temperature (T_s) is then calculated by solving (4) using iterative techniques.

b. Biosphere model

The biosphere model used for the verification and intercomparison studies is the Simplified Simple Biosphere (SSiB) Model of Xue et al. (1991). It is based upon the Simple Biosphere Model (SiB) of Sellers et al. (1986) but with reduced computational complexities of the diurnal variation of surface albedo and of stomatal and aerodynamic resistances. The terms "simplified" and "simple" are both misnomers, as SSiB is still quite complex, with 23 parameters that must be specified.

The subsurface of the model contains three interactive soil layers with the depth and porosity of each soil layer dependent upon surface vegetation type. Water is allowed to diffuse between each of the subsurface layers and drain out of the lowest layer as subterranean runoff. Runoff in SSiB occurs both on the surface and from the bottom layer. Surface runoff occurs only with infiltration excess. The spatial nonuniformity of rainfall is taken into account in this overland flow calculation. In the bottom layer, besides infiltration excess, gravitationally driven drainage also contributes to water loss to groundwater (Sato et al. 1989).

As in the bucket, if the surface temperature is below freezing when precipitation reaches the ground, it is assumed to be snow and accumulates on the ground. When the temperature rises above freezing, snow melts. The water then either infiltrates into the soil layer or goes into surface runoff, depending on whether the temperature of the third (deep soil) layer is above or below freezing. This criterion apparently produces behavior unlike the observations, as will be seen later.

The two uppermost soil layers are designed to be the root-active zone of the subsurface with water transpiration rates governed by the stomatal resistances of the surface vegetation. The uppermost soil layer can also directly evaporate into the air.

The surface vegetation types of SSiB can vary from mixtures of broadleaf, needleleaf, deciduous, and evergreen trees to broadleaf shrubs with or without ground cover to just ground cover (grass) or bare soil. The SSiB surface vegetation scheme also contains a "winter wheat" type to account for agricultural regions. With each vegetation type, resistances to evapotranspiration and sensible heat flux are calculated according to atmospheric and subsurface conditions. In addition, canopy water storage is maintained. The canopy water storage is increased by precipitation interception and decreased by direct evaporation and drainage from the leaves. Since the meteorological, actinometric, and soil moisture measurements used in this study were taken within a grass plot, the grass cover vegetation type was selected for the experiments involving SSiB.

5. Bucket and SSiB model intercomparison

a. Theoretical framework for intercomparison

To compare the soil moisture calculations for SSiB and the bucket models and the observations, two issues must be addressed: representation of available soil moisture and vertical resolution. The observations and bucket model both deal with available soil moisture, while SSiB calculates soil wetness. As seen in Fig. 3, the observations for our six stations are for the layers 0–10, 10–20, 20–50, and 50–100 cm, while SSiB has three layers, 0–2, 2–49, and 49–149 cm, and the bucket considers only one layer, 100 cm.

Figure 5 shows for our six stations the 6-yr average measured W for the 0–50- and 50–100-cm layers. For all the stations, there is more water in the top (0–50 cm) layer than the bottom, except for Yershov and Uralsk in the summer, when both layers are very dry. For the stations for which we have data (Table 1), the field capacity of the top layer is higher than that of the lower half, so this is not unexpected. The top layer also has a larger seasonal cycle at all the stations. For Uralsk and Ogurtsovo, the W in the bottom layer is virtually constant for the entire year, so that comparisons with model output for the top 50 cm would capture virtually all of the variations at these stations. For the other stations, however, there are also large variations in the bottom half of the top meter.

Instead of available soil moisture, the SSiB model uses a soil wetness fraction defined as the ratio of total soil moisture storage to its total water-holding capacity. Because both the observations and the bucket use W, comparisons with SSiB will be most convenient if this parameter can also be derived from SSiB output. This can be done if certain physiological characteristics of the soil and the vegetation are known. For a given subsurface layer of SSiB (Xue et al. 1991),

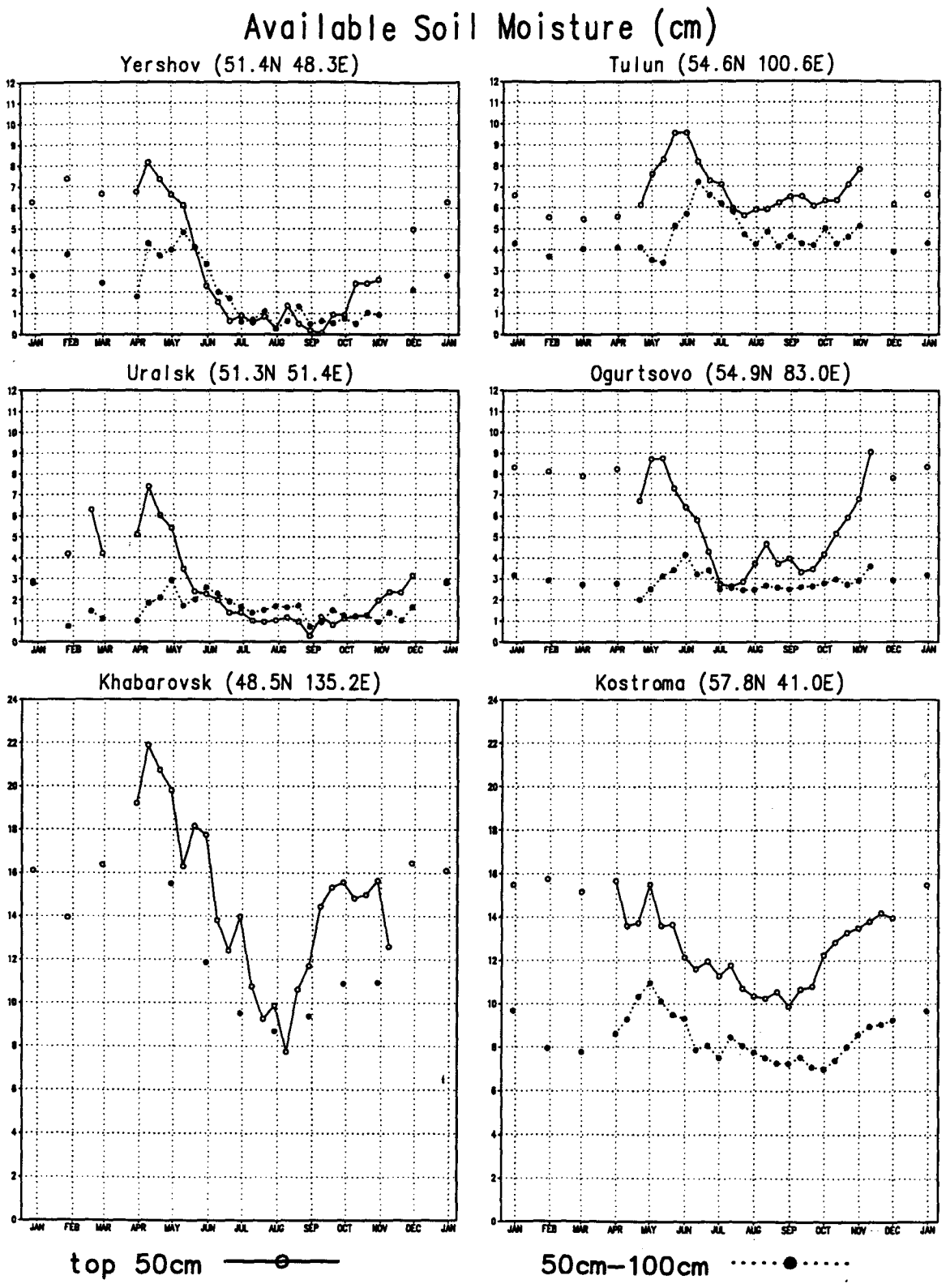

FIG. 5. The 6-yr average (1978–1983) seasonal cycle of observed available soil moisture in the top two 0.5-m layers for the six stations (Fig. 1, Table 1). The abscissa labels indicate the beginning of the months. The data points taken every 10 days during the growing season are connected with lines. The other data points represent end of the month measurements.

$$W_{0_i} = S_i P_i D_i, \tag{10}$$

where W_{0_i} is total soil moisture of ith layer, S_i is soil wetness fraction of ith layer, P_i is porosity of the ith layer = 0.42 for all layers, and D_i is thickness of the ith layer.

The inferred wilting level of SSiB is S_i, which equals 0.32 for all layers, as resistance to transpiration reaches ∞ at this level of wetness. The value of S_i may go slightly lower in the top layer if bare soil evaporation exceeds water input. Available soil moisture W_i for the ith subsurface layer of SSiB is then

$$W_i = (S_i - 0.32)P_i D_i. \tag{11}$$

In SSiB, the two uppermost subsurface layers plus 1% of the third layer are the root-active regions, and thus, water can be extracted by the vegetation within these layers (Fig. 3). Moisture in the third layer can be extracted by vegetation, but more much slowly than from the top two layers since root extraction is minimal and diffusion must move water from the third layer into the second layer and then into the roots. If we turn off precipitation and run SSiB with typical station data as forcing, all three layers end up with S_i close to 0.32. Since in SSiB, if $S_i > 0.64$, rapid gravitational drainage will remove moisture, SSiB for grass cover (the only surface type considered in this paper) has an effective field capacity of 6.6 cm [$(0.64 - 0.32) \times 0.42 \times 49$ cm] for the top two layers combined and 13.4 cm [$(0.64 - 0.32) \times 0.42 \times 100$ cm] for the third layer.

Another way of stating this is to say that embedded in SSiB is a 20.0-cm bucket representing the top 1.49 m of soil divided into two compartments. The water content, however, can exceed field capacity if the precipitation rate is greater than the combined rates of downward diffusion, evapotranspiration, and gravitational drainage.

Because of the inconsistent vertical resolutions, there are several possible methods for comparing available soil moisture (W) for SSiB, the bucket, and the observations. A direct comparison between the observations for the top 50 cm and W from the top two layers of SSiB (top 49 cm) is obvious and clear, and we will use this method. But the bucket model calculates W only for the entire top 1 m. One option is to compare these top 50-cm values of W with dW_{bucket}, where $d = 0.5$, but as can be seen in Fig. 5, more than one-half the soil moisture resides in the top 50 cm for all stations. Another option is to calculate d from the observations for each station (each month or annual average) and then compare dW_{bucket} with the top 50-cm W for the observations and SSiB. This would impart physical meaning to d, which is different for each station and absent in both models, so for one comparison we will simply directly compare the top 50 cm and W from the top two layers of SSiB with $0.5W_{\text{bucket}}$, keeping in mind that this does not accurately reflect the physics of the bucket model.

Because we also have observations of W for the top 1 m of soil and this quantity is directly calculated by the bucket, we will also make this direct comparison. But the 1-m depth bisects the third SSiB layer. Therefore, to compare the 1-m bucket output with SSiB, we again must choose from one of several options. Three possibilities are 1) using twice W from the top two SSiB layers, 2) using the total of the three SSiB layers, keeping in mind that they cover 1.5 m instead of 1 m; or 3) using W from the top two SSiB layers plus one-half W from the third layer. We ran our SSiB simulations for all six stations calculating the output using all three of these methods. Figure 6 shows the 5-yr average output for the last 5 yr of the 6-yr simulations for three of the stations compared to the 1-m observations and the bucket results. We excluded the first year to avoid any spinup problems, as discussed in the next section. For each station, a different method produces a better comparison with observations, and there is no clear best method for doing the comparison. Be-

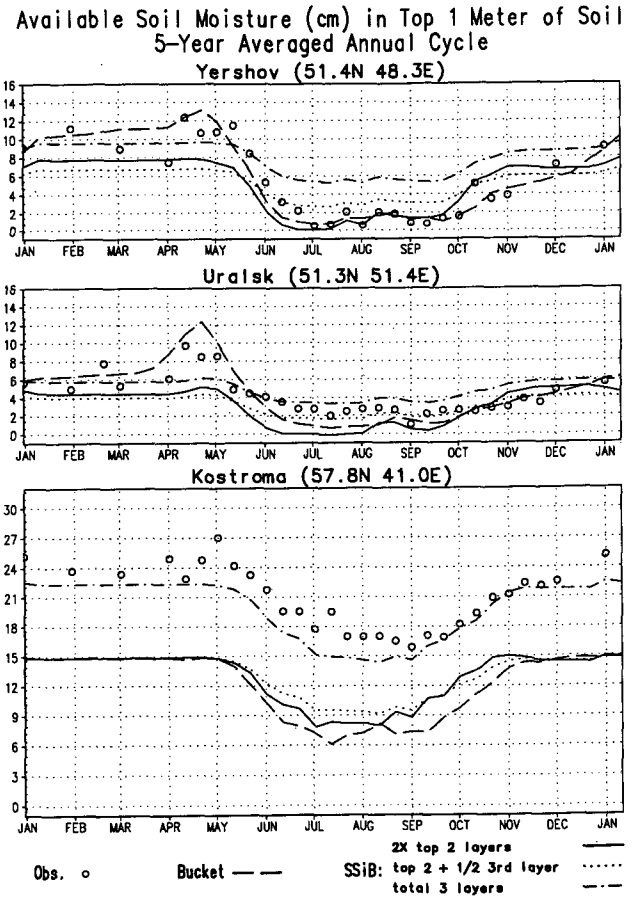

FIG. 6. Comparison of three methods of comparing 1-m SSiB results with observations and bucket results at three different stations, with results averaged over the last 5 yr of the 6-yr simulations.

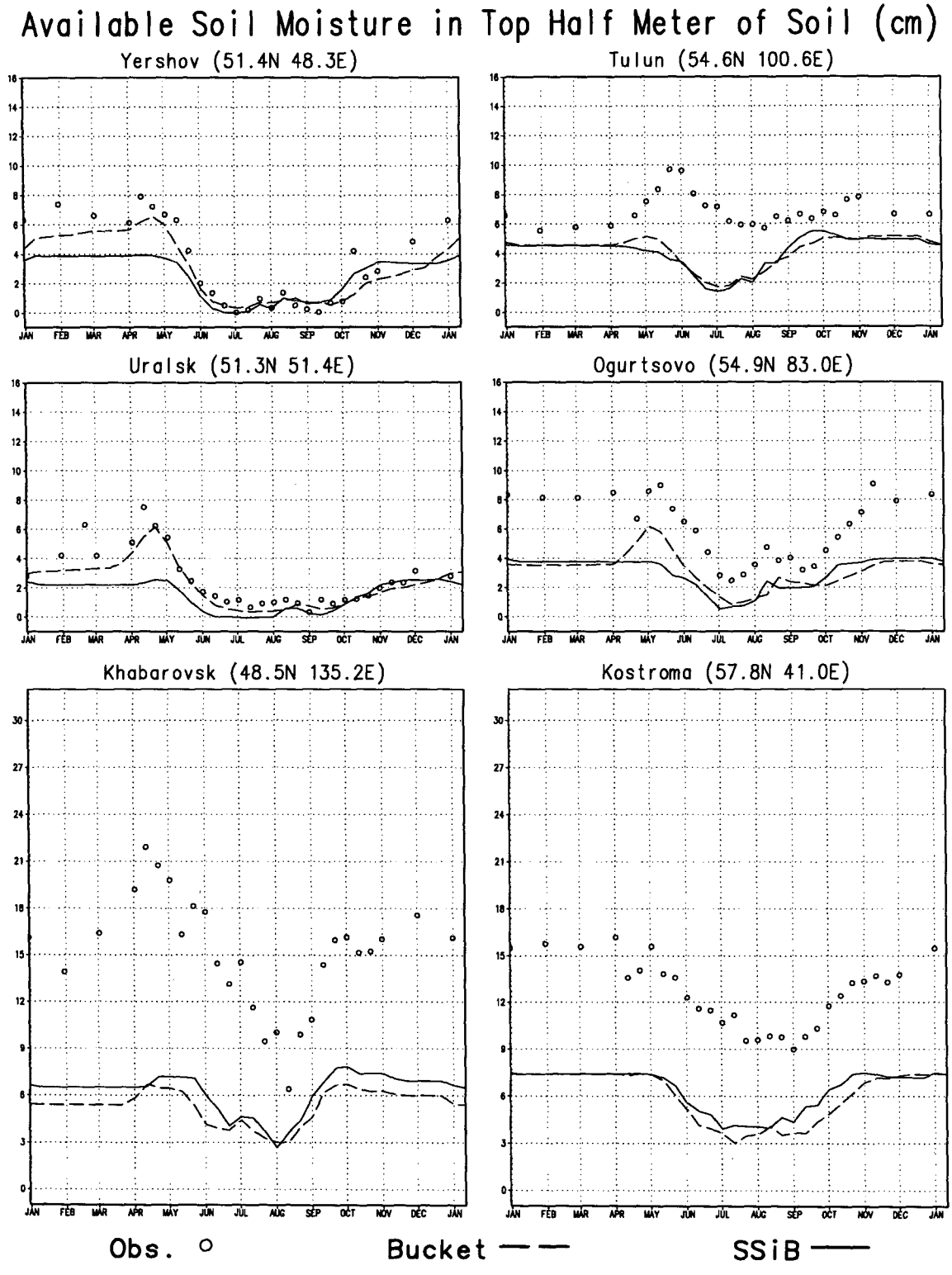

FIG. 7. Results of simulations for available soil moisture in top 0.5 m as compared to observations for all six stations, averaged over the last 5 yr of the 6-yr simulations (1979–1983). One half of the 1-m W from the bucket is compared to observations for the top 50 cm and total W from the top two SSiB layers, with a total depth of 49 cm.

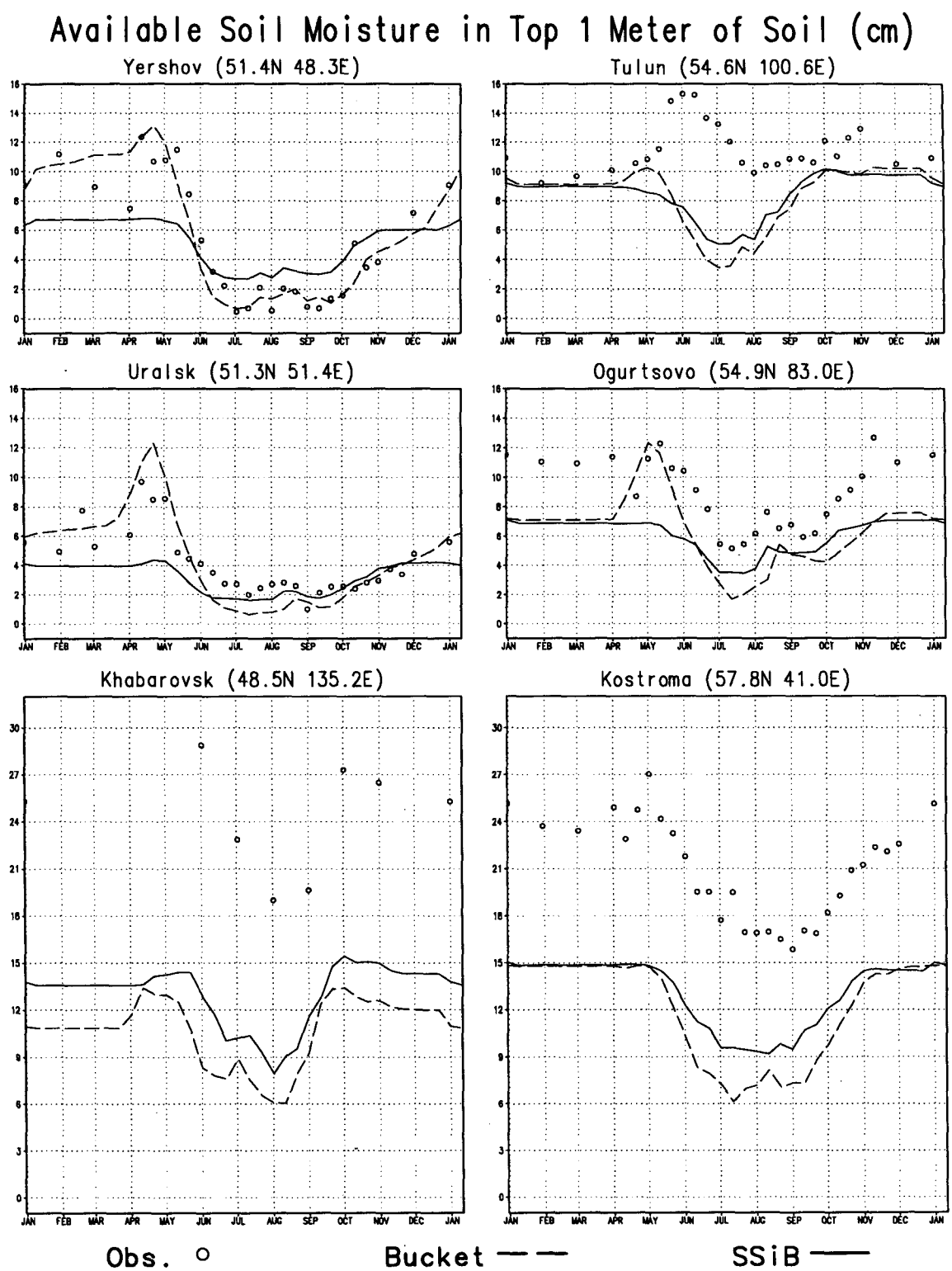

FIG. 8. Results of simulations for available soil moisture in the top 1 m as compared to observations for all six stations, averaged over the last 5 yr of the 6-yr simulations (1979–1983). The 1-m W from the bucket is compared to observations for the top 1 m and total W from the top 2 SSiB layers plus half the W from the bottom SSiB layer.

TABLE 2. Soil moisture statistics for SSiB and bucket model output compared to observations for 0–50-cm depth.

Model	Yershov	Uralsk	Ogurtsovo	Kostroma	Khabarovsk	Tulun
			Correlations of 5-yr run			
SSiB	0.85	0.58	0.88	0.86	0.62	0.28
Bucket	0.93	0.78	0.77	0.83	0.66	0.31
			Biases of 5-yr run (cm)			
SSiB	*−0.6*	*−0.7*	*−2.7*	*−6.0*	*−8.4*	*−2.8*
Bucket	*0.0*	*0.1*	*−2.4*	*−6.4*	*−9.3*	*−2.7*
			Winter rms errors and bias (cm)			
SSiB	2.8	3.2	4.1	7.7	9.0	1.5
	−3.0	*−2.1*	*−4.3*	*−8.2*	*−8.9*	*−1.4*
Bucket	1.6	2.3	4.3	7.7	9.8	1.5
	−2.0	*−1.3*	*−4.6*	*−8.2*	*−10.0*	*−1.3*
			Spring rms errors and bias (cm)			
SSiB	2.4	2.8	4.3	7.4	11.5	3.0
	−2.5	*−2.6*	*−4.2*	*−7.1*	*−12.4*	*−3.8*
Bucket	1.3	1.4	3.6	7.8	12.2	2.8
	−0.8	*−0.6*	*−3.3*	*−7.2*	*−13.3*	*−3.4*
			Summer rms errors and bias (cm)			
SSiB	0.2	0.8	2.3	5.6	6.5	3.7
	−0.2	*−0.8*	*−2.4*	*−6.0*	*−6.9*	*−4.1*
Bucket	0.2	0.5	2.0	6.3	7.3	3.7
	0.0	*−0.4*	*−2.1*	*−6.6*	*−7.4*	*−4.0*
			Fall rms errors and bias (cm)			
SSiB	0.4	0.5	2.5	5.3	8.0	1.8
	0.2	*−0.2*	*−2.6*	*−5.7*	*−8.1*	*−1.8*
Bucket	1.0	0.5	2.8	5.9	8.9	1.9
	−0.5	*−0.4*	*−3.0*	*−6.5*	*−9.1*	*−2.0*

Correlations are of 10-day averages between model output and observations for entire 5-yr period.
Rms errors are for seasonal means.
Bias is model output *minus* observations.
Bias measurements are indicated by italic font.
Seasons are the conventional definitions: winter (December–January–February), spring (March–April–May), summer (June–July–August), and fall (September–October–November).

cause the total of the three layers is for a depth inconsistent with the observations and the bucket, and because we will separately compare the top two layers with the observations for the top 50 cm, we choose to use the top two layers plus one-half of the third for the comparisons with the 1-m observations and bucket output, keeping in mind that there are other possibilities.

The available soil moisture intercomparison will then be made in two ways: 1) top 50-cm observations with the top two layers of SSiB and with one-half of the bucket and 2) top 1-m observations with the top two layers of SSiB plus one-half of the third layer and with the entire bucket. The first method should favor SSiB and the second favor the bucket, while allowing intermodel and observational comparisons. Along with the soil moisture analysis, comparisons will be made between each model's calculations of hydrological and energy-flux components, as well as direct comparisons of model outputs with observed values of albedo, net radiation, and water-equivalent snow cover depth.

b. Intercomparison results

As described previously, for each station, the models were initialized with observed soil moisture and run for 6 years forced with observed data. For two of the stations, Kostroma and Khabarovsk, observations showed initial W to be greater than 15 cm, so for the bucket model these simulations were started with W = 15 cm. For SSiB, S_i was set equal to the observed values using (11).

Although we started the calculations with observed values of soil moisture, these values are not in equilib-

TABLE 3. Soil moisture statistics for SSiB and bucket model output compared to observations for 0–1-m depth.

Model	Yershov	Uralsk	Ogurtsovo	Kostroma	Khabarovsk	Tulun
			Correlations of 5-yr run			
SSiB	0.80	0.57	0.87	0.87	0.50	0.23
Bucket	0.90	0.76	0.79	0.81	0.48	0.15
			Biases of 5-yr run (cm)			
SSiB	*0.1*	*−0.6*	*−2.7*	*−7.5*	*−11.2*	*−3.2*
Bucket	*1.0*	*0.7*	*−2.4*	*−8.6*	*−13.6*	*−3.2*
			Winter rms errors and bias (cm)			
SSiB	3.2	2.4	3.9	8.5	—	1.3
	−3.3	*−1.9*	*−4.1*	*−9.2*	—	*−0.9*
Bucket	1.2	1.2	3.8	8.5	—	2.0
	−0.2	*0.2*	*−4.0*	*−9.3*	—	*−0.7*
			Spring rms errors and bold (cm)			
SSiB	3.0	3.5	4.1	9.7	12.3	2.8
	−2.6	*−2.9*	*−3.8*	*−9.8*	*−21.1*	*−3.6*
Bucket	0.7	2.4	2.4	10.7	13.6	3.1
	0.5	*1.2*	*−1.9*	*−10.2*	*−23.3*	*−3.1*
			Summer rms errors and bias (cm)			
SSiB	1.5	0.9	2.1	7.3	9.8	5.2
	1.4	*−0.7*	*−2.3*	*−7.9*	*−10.5*	*−5.6*
Bucket	0.2	1.4	3.0	9.7	12.3	6.2
	−0.3	*−1.4*	*−3.2*	*−10.4*	*−13.0*	*−6.8*
			Fall rms errors and bias (cm)			
SSiB	1.7	0.8	2.4	6.4	11.0	2.2
	1.6	*0.1*	*−2.6*	*−6.9*	*−12.3*	*−1.7*
Bucket	1.0	0.9	2.8	7.3	13.0	2.6
	0.1	*−0.3*	*−3.1*	*−8.3*	*−14.1*	*−1.6*

See Table 2 for definitions.

rium with the values the models would like to calculate. To examine the potential influence of spinup on our results, we recalculated all the simulations starting with $W = 0$ cm and $W = 15$ cm. By comparing these results to the original simulations, we can see the influence of initial conditions on the results; however, the initial simulations may still contain spinup error in the first year. Therefore, we also restarted each simulation at the beginning of each year (1979–1982) and compared the results to the original simulations. By examining the differences in all these experiments, we determined that large errors in the bucket initial conditions persisted only for a few months, in agreement with the autocorrelation timescales as determined by Vinnikov and Yeserkepova (1991) from soil moisture observations in the former Soviet Union. SSiB, however, had a longer memory, especially for dry initial conditions, when differences persisted for several years. This was due to the slow rate of change of soil moisture in the third model layer, which is isolated from the surface by the two layers above it. A detailed analysis of this behavior is beyond the scope of this paper. Since for our stations the only difference between model values and initial observations was that the observations were too wet, this dry persistence of SSiB is not a problem if we exclude the first year of our simulations. Therefore, we exclude the first year of our simulations in calculating statistics and comparing average seasonal cycles of results and compare 5-yr averages of the last 5 yr of the 6-yr simulations with averages for the same 5 yr from the data.

The 5-yr average annual cycle results for all six stations for the 50-cm comparison are shown in Fig. 7, and for the 1-m comparison are shown in Fig. 8. Quantitative measures of the agreement of each simulation with observations are given in Tables 2 and 3. It can be seen in both the figures and tables that the results are highly station dependent and also depend on the season. For both Khabarovsk and Kostroma, both models are much too dry but capture the phase of the seasonal cycle. For Yershov and Uralsk, both models produce quite good simulations, except SSiB

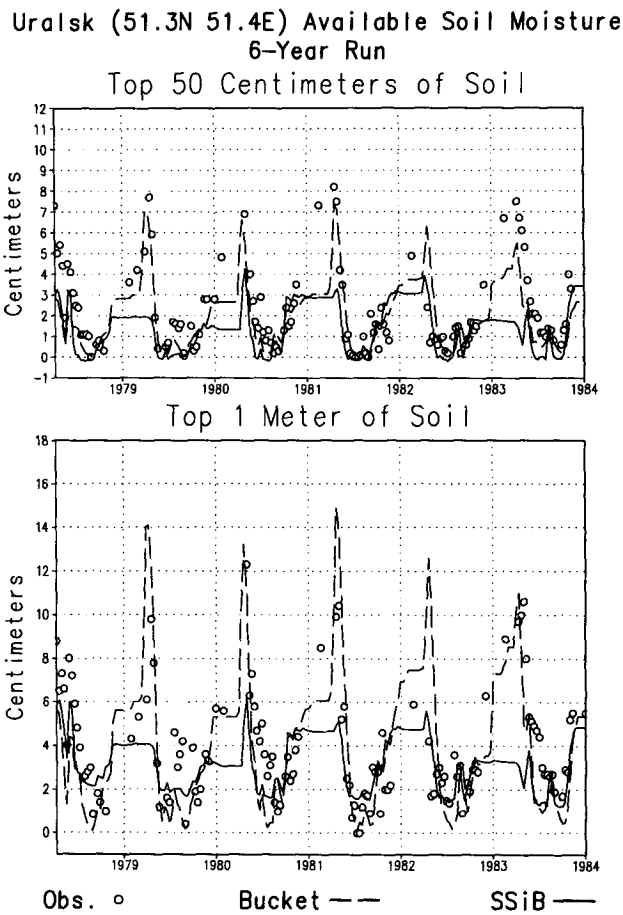

FIG. 9. Simulations and observations of available soil moisture for Uralsk for 1978–1983, shown as 10-day averages. See Figs. 7 and 8 for the 1979–1983 average seasonal cycle. The abscissa labels indicate the beginning of the years.

does not capture the spring peak produced by snow melting, and for Yershov, SSiB is too wet in the 1-m comparisons for summer and fall and too dry in the 50-cm comparisons for winter and spring. For Ogurtsovo, both models do a good job but are too dry. For Tulun neither model agrees with the observations. For the stations without large biases or phase errors, Yershov and Uralsk, both models have about the same accuracy. SSiB is clearly not better than the bucket at producing correct soil moisture but, as is demonstrated below, can produce quite different heat fluxes. Detailed intercomparisons for each station follow.

1) URALSK, OGURTSOVO, AND YERSHOV

Uralsk, Ogurtsovo, and Yershov all had similar results, although Ogurtsovo simulations were slightly too dry, and so will be discussed as a group, with Uralsk as an example. They are all from the same hydrological regime, in the dry center of the continent. Figure 9 shows the soil moisture results for 1978–1983 for Uralsk, which can be compared with the 1979–1983 averages of these results shown in Figs. 7 and 8. Both model results and observations show a similar annual pattern of soil moisture with a drying during the summer and a replenishing of moisture during the fall. This is in spite of relatively uniform precipitation all year long (Figs. 10 and 11). The seasonal cycle of soil moisture is therefore clearly driven by seasonal variations of the various components of the hydrological cycle, not the direct forcing due to precipitation.

During the springtime snowmelt, the bucket model gives a much better simulation, with the spike of soil moisture being quite well simulated, while this spike is absent in the SSiB results (Fig. 9). SSiB's response to snowmelt is most likely a result of its runoff parameterization. SSiB partitions all of the snowmelt into runoff as long as its deep soil temperature is below freezing, and in nearly all cases during snowmelt, the deep soil temperature of SSiB was below freezing in the spring, causing runoff rather than soil moisture replenishment.

The differences between SSiB and the bucket model described above are quite similar to some of the findings for the northern Canada region of Henderson-Sellers

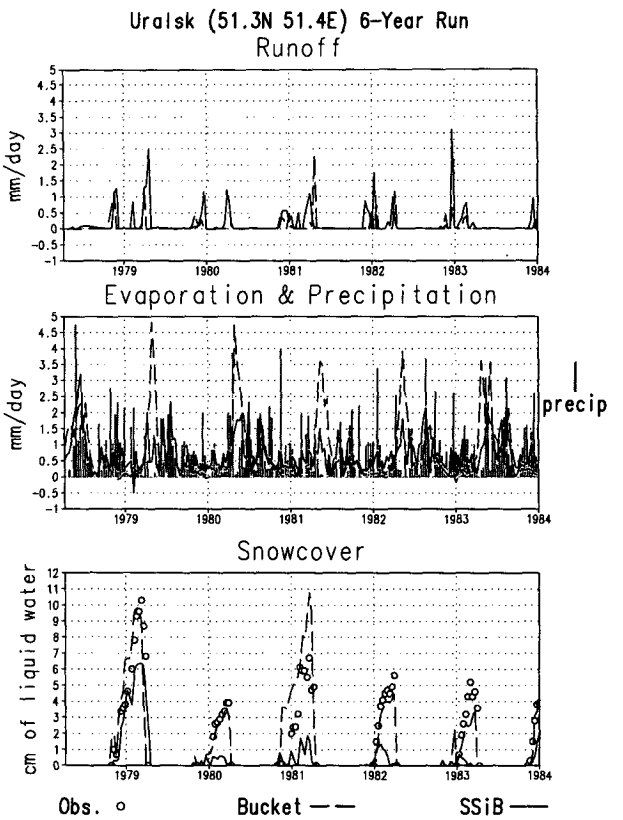

FIG. 10. Components of the hydrological budget for Uralsk simulations in Fig. 9, shown as 10-day averages. For runoff and evaporation, only simulations are available. Observed precipitation, used as forcing in the simulations, is shown. For snow cover, simulations and observations are shown.

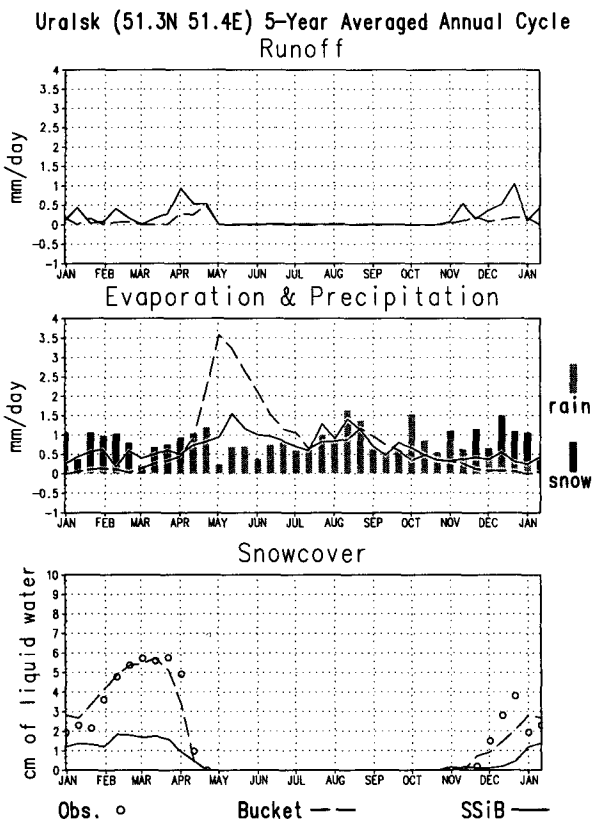

FIG. 11. The 5-yr average seasonal cycles of components of the hydrological budget for Uralsk simulations shown in Fig. 10.

et al. (1990), who compared the hydrology output of the BATS scheme [Dickinson et al. (1986)—a biosphere-type model] with that of the GFDL bucket model for different regions of the globe. However, observations of soil moisture were unavailable to them.

Because SSiB partitions a much higher fraction of its snowmelt into runoff, in most cases it produced higher amounts of runoff during the spring snowmelt (Figs. 10 and 11). Even though the bucket model produced far more snow cover, and hence snowmelt, during the preceding winter than did SSiB, the snowmelt filled the bucket rather than producing runoff. For all the stations, the bucket produces an excellent snow cover simulation, while SSiB consistently simulates too little snow cover.

During the middle and late spring, the bucket model's evaporation (actually evapotranspiration) rates were approximately 0.5–2.0 mm day^{-1} higher than SSiB's (Fig. 11). The increased spring evaporation from the bucket model is also seen in the surface heat flux analysis (Fig. 12). Latent heat flux from the bucket exceeds that of SSiB by 20–50 W m^{-2} during the middle and late spring, more than double that of SSiB. In the winter, the SSiB latent heat flux is close to 20 W m^{-2}, while that of the bucket is close to 0. Only when snow is melting and saturating the surface does the evaporation from one model differ from that of the other.

In addition, a complementary difference of sensible heat flux between the two models is seen (Fig. 12). From late spring through the fall, SSiB's sensible heat flux is about 20 W m^{-2} higher than the bucket's. The lower latent heat flux in spring and higher amounts of sensible heat flux later produced by SSiB are consistent with the results of Sato et al. (1989). In spite of quite similar soil moisture simulations in the early summer, the latent and sensible heat fluxes are very different. Because of this, if a GCM changed the choice of land surface parameterization from one of these models to the other, there would probably be large effects on the simulated climate.

Along with differences in heat flux calculations, SSiB and the bucket model show some modest disagreement in their radiative flux calculations, even though they were forced by identical downward shortwave and longwave radiation. In addition to soil moisture and

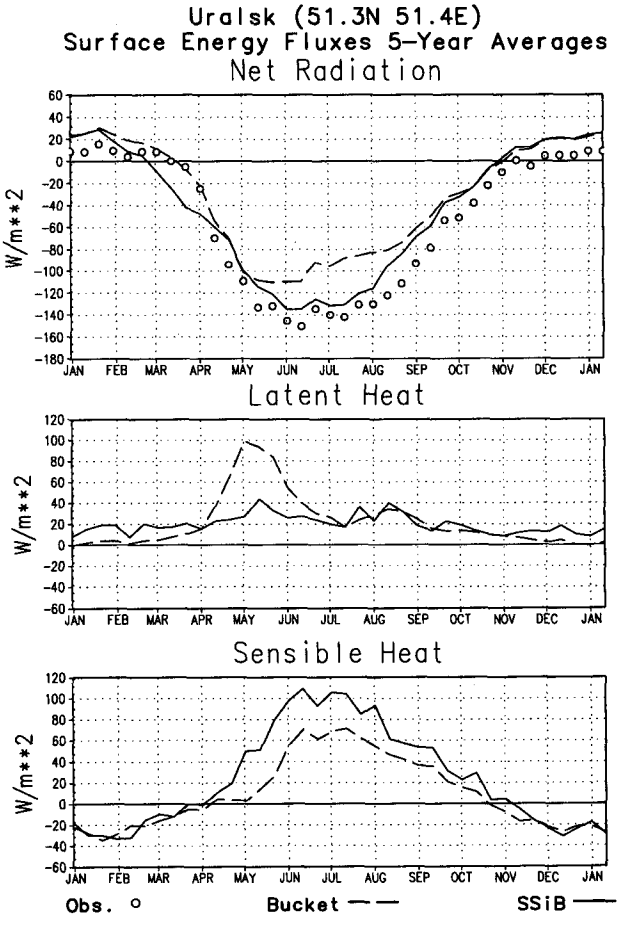

FIG. 12. The 5-yr average seasonal cycles of simulated components of the surface energy fluxes for Uralsk simulations shown in Fig. 9, shown as 10-day averages. Also shown are observations of net radiation. For all fluxes, upward is positive.

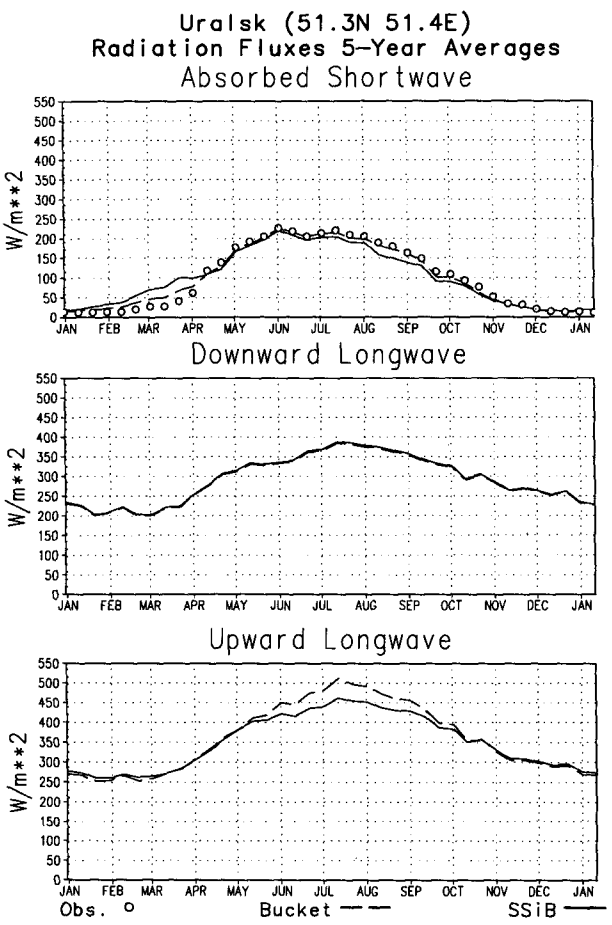

FIG. 13. The 5-yr average seasonal cycles of components of the surface radiative fluxes for Uralsk simulations shown in Fig. 9. Also shown are observations for absorbed solar radiation. For this figure only, all fluxes, whether upward or downward, are shown as positive.

snow cover, we can use the net radiation and albedo/absorbed shortwave radiation as independent verification of these calculations. The net radiation observations (Fig. 12) show disagreements with the SSiB results in the spring and the bucket results in the summer. The spring discrepancy can be traced directly to the poor snow simulation by SSiB, which results in much more absorbed shortwave radiation (Fig. 13). As seen in Fig. 14 for Uralsk, SSiB produces albedos approximately 0.10–0.20 lower than the bucket model during the winter, which is likely a result of the lower amounts of snow cover produced by SSiB.

During the warmer months, the bucket model produces lower albedos than SSiB (~0.05–0.10), which explains the higher amounts of absorbed shortwave radiation by the bucket. In addition, for all of the stations an increase in SSiB's calculated albedo occurs during the end of each summer season, because SSiB assumes that at the end of each summer the grass cover dries up, increasing the albedo (Justice et al. 1985). This behavior of albedo, however, is not seen in the observations for any of the stations in our dataset. In fact, throughout the entire year, the bucket model's albedos and absorbed solar radiation appear to be in better agreement with observations than SSiB's. Since the surface albedo in SSiB is decided by the vegetation parameters, it appears that the vegetation parameters that SSiB uses for grassland may not be a proper representation for the Russian regions we studied.

The bucket produces more upward longwave radiation during the summer than SSiB (Fig. 13), and this could account for the differences in net radiation (Fig. 12). This difference also agrees with the lower sensible heat flux seen in Fig. 12. The way the bucket calculates surface temperature and partitions the outgoing energy is different in the summer than the way it is done in SSiB, but with the data here, we cannot definitively say which is more correct.

2) KOSTROMA AND KHABAROVSK

Kostroma and Khabarovsk, both in wet regions of Russia, had similar results, and Kostroma will be used as an example. Figure 15 shows the soil moisture results for 1978–1983 for Kostroma, which can be compared to the 5-yr (1979–1983) averages of these results shown in Figs. 7 and 8. The annual cycles of soil moisture produced by SSiB and the bucket model are quite similar for both stations. Drying of the soil occurs during the summer, followed by a complete saturation in early fall that carries through to the following summer. The saturation of both models during the fall is due to the moderate amounts of rainfall that exceed calculated evaporation rates (Fig. 16). The snow cover and frozen

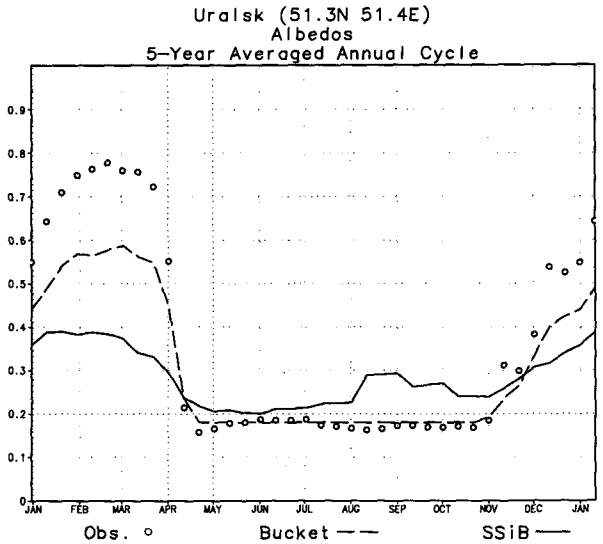

FIG. 14. Simulated and observed albedos for Uralsk simulations shown in Fig. 9, shown as 10-day averages of 5-yr average seasonal cycles.

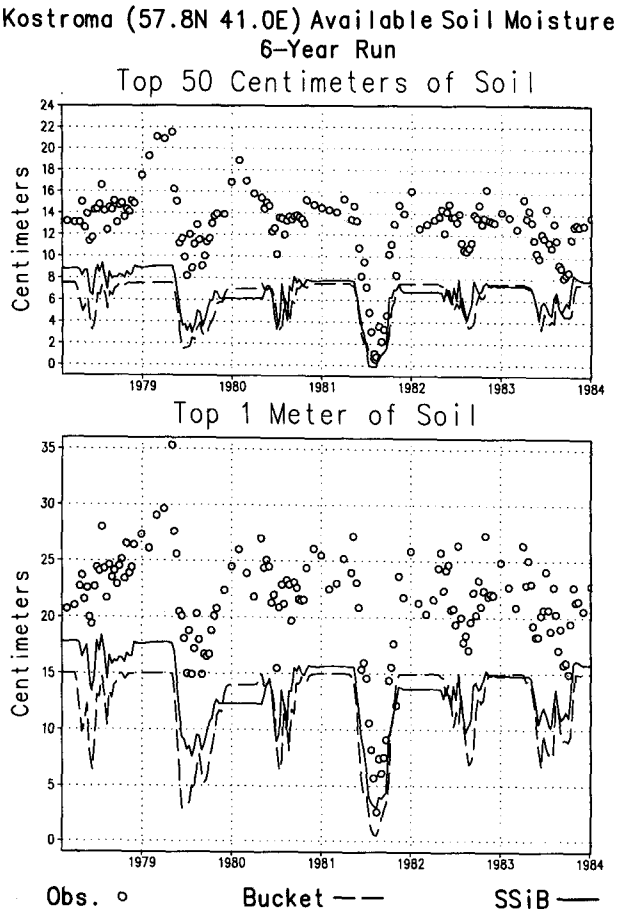

FIG. 15. Simulations and observations of available soil moisture for Kostroma for 1978–1983, shown as 10-day averages. See Figs. 7 and 8 for the 1979–1983 average seasonal cycle.

conditions of the winter then act to sustain the soil saturation.

Observations show soil moisture is persistently higher than the calculated values and is more variable for these stations during the fall, winter, and spring. Because both SSiB and the bucket model are completely saturated during the fall, winter, and spring, they cannot exhibit any sort of variability or attain any of the higher values of soil moisture that are observed. During the summer of 1981, when there was very little precipitation, both models actually do a good job of simulating W (Fig. 15). These results suggest that the prescribed model field capacities are too low as the water table is too deep to influence the soil moisture in the top 1 m.

Both models simulate the snow cover quite well (Fig. 16), but in SSiB there is an incorrect lag of about half a month. Because of the saturated conditions in the winter, both models put all the snowmelt into similar spring runoff peaks (Fig. 16) with the same time lags as snowmelt. In contrast to Yershov, Uralsk, and Ogurtsovo, runoff in the SSiB simulation continues throughout the summer, and both models produce another peak in the late fall and early winter. All these components of the hydrological cycle might be different if the soil moisture simulations were more accurate and soil wetness were less.

The net radiation is fairly well simulated by both models (Fig. 17), except for too high values in the winter, due to too low albedos, and slightly too low values for the bucket in the summer. Summer latent and sensible heat fluxes (Fig. 17) are quite similar for both models, in contrast to the stations discussed earlier (Fig. 12). In the spring, however, there are large differences.

3) TULUN

Perhaps the most interesting results are for Tulun (Fig. 18). Both SSiB and the bucket model consistently dry the soil during the summer and replenish moisture into the soil in the late summer and fall, when precipitation increases. However, the observations show soil moisture to be quite variable from year to year and not well correlated with either of the models. In some

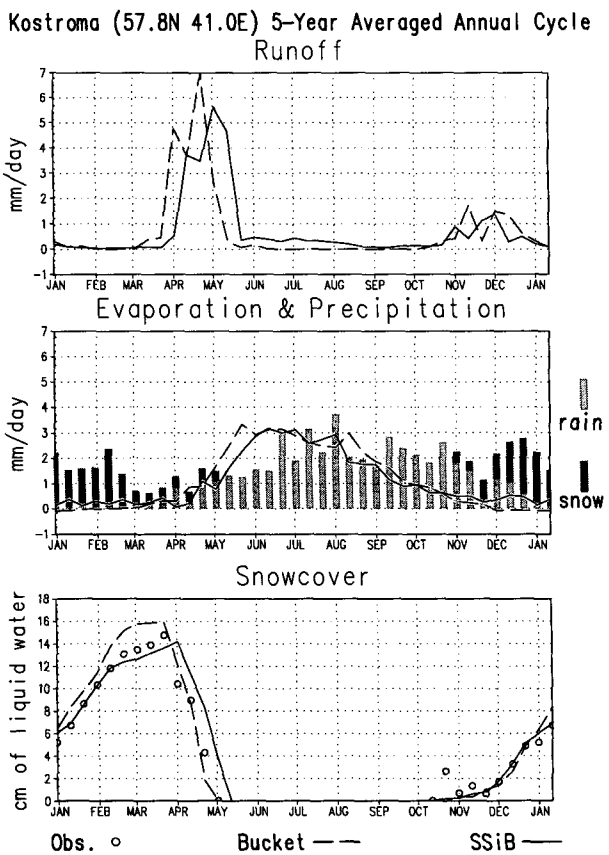

FIG. 16. Components of the hydrological budget for Kostroma simulations shown in Fig. 15, shown as 10-day averages of 5-yr average seasonal cycles. See caption of Fig. 10 for further details.

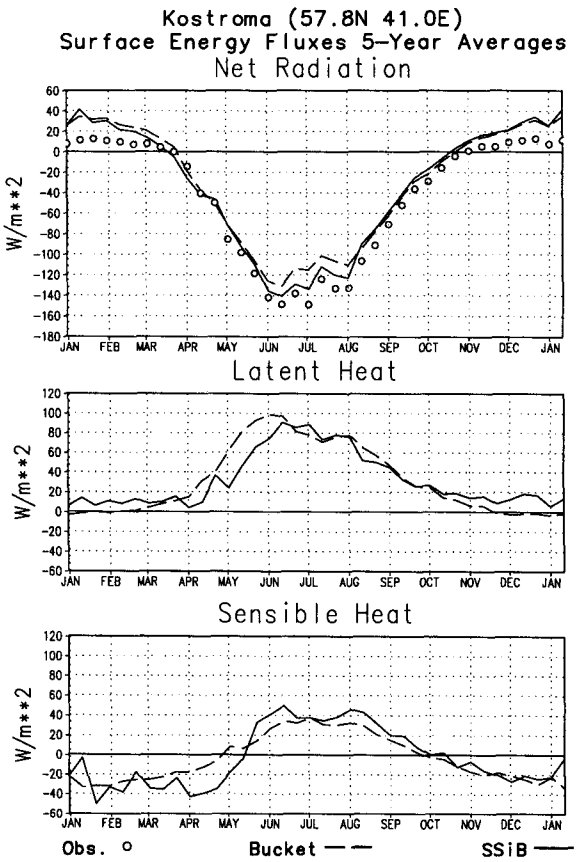

FIG. 17. The 5-yr average seasonal cycles of components of the surface energy fluxes for Kostroma simulations shown in Fig. 15, shown as 10-day averages. Also shown are observations of net radiation. For all fluxes, upward is positive.

instances, the models dry the soil while observations show no such drying or even increases of soil moisture (e.g., summers of 1981 and 1983). Averaged over the five years (Figs. 7, 8), the annual cycle of SSiB and the bucket model's soil moisture appear to be fairly consistent. However, the observed annual cycle bears little resemblance to the models. The statistics in Tables 2 and 3 clearly support these statements.

With the data available to us, we can only speculate about the reasons for these discrepancies. Tulun has a seasonal cycle of precipitation completely dominated by the summer monsoon (Fig. 19). Snow cover and latent heat simulations in the spring by each model are similar to those of Uralsk (Fig. 11), so antecedent conditions do not appear to contribute to the very different summer skills (Tables 2 and 3). Perhaps in a situation with such large snowmelt followed by heavy rains, more detailed consideration of subsoil hydrology is required. Water table data for this station show the water table to be deeper than 20 m at this station (Table 1), so water table variations cannot explain the discrepancies. The observations were taken in a clearing in a forest, so biological factors may be present in the observations.

6. Discussion and conclusions

We can reach several conclusions from the results presented above. Comparison of soil moisture simulations with actual observations is crucial to test the validity of the parameterizations and discover the reasons for discrepancies. We need full sets of hydrological data for many years and many stations to test the models. Individual years from particular stations can show particularly bad or particularly good simulations, but only by examining many stations and many years can general conclusions be reached. The Russian dataset used in this paper, while incomplete, is invaluable for this work.

Differences between the bucket and SSiB and between each and the observations could be explained by different model treatments of energy fluxes, soil water, the canopy, or the diurnal cycle, and the prescription of vegetation parameters in SSiB. In this paper, we do not have enough verification data (only soil moisture, albedo, snow cover, and net radiation, but not separate longwave fluxes, runoff, or sensible and latent heat fluxes) to definitively explain all these differences. We are working with the data from Valdai,

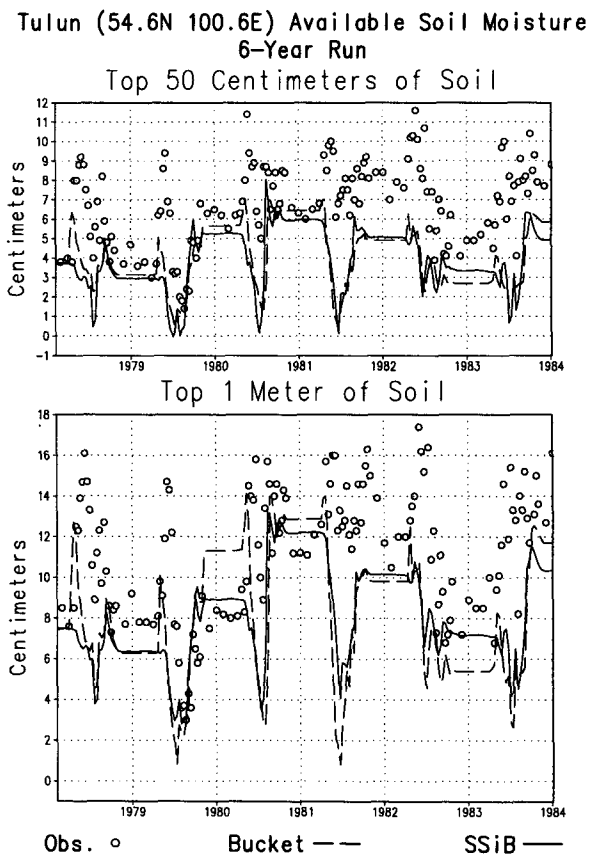

FIG. 18. Simulations and observations of available soil moisture for Tulun for 1978–1983, shown as 10-day averages. See Figs. 7 and 8 for the 1979–1983 average seasonal cycle.

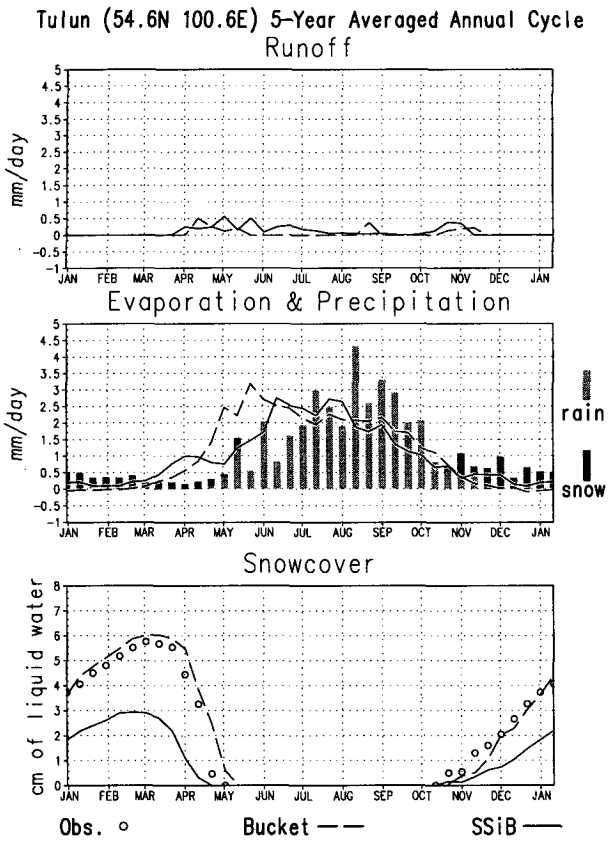

FIG. 19. Components of the hydrological budget for Tulun simulations shown in Fig. 18, shown as 10-day averages of 5-yr average seasonal cycles. See caption of Fig. 10 for further details.

Russia, which are much more comprehensive than data from the other regions, to further answer some of these questions in the future.

Both SSiB and the bucket have serious deficiencies in their simulation of soil moisture in the midlatitudes. Both models were too dry in some regions at all times (Kostroma and Khabarovsk). In these regions, using the correct field capacity would probably improve the simulations by both models. Both models had an albedo that was too low in the winter, but this was not important for the soil moisture simulations as there was little insolation then. It may be important, however, in simulating the exact timing of the spring snowmelt. In addition, SSiB failed to properly model the soil moisture increase during the spring snowmelt and had an erroneous increase of albedo during the second half of the summer.

The SSiB and bucket simulations are quite similar to each other when forced with observations because SSiB implicitly contains a bucket. Neither model has large biases compared to the other. This is in spite of the fact that SSiB explicitly models stomatal resistance and the diurnal cycle while the bucket does not.

There is no evidence in the experiments here that either SSiB or the bucket is superior in its soil moisture calculations. The latent heat, sensible heat, runoff, and radiative fluxes, however, can be very different depending on which model is used.

The results of these calculations could clearly be improved by adjusting the parameters and modeling assumptions used for SSiB and the bucket. In this paper we specifically tested versions used in past and current GCM work, so that published results with these models can be evaluated. We could have tuned each model to the same vertical resolution or modified the frozen soil treatment to SSiB, for example, to isolate different processes. That work is beyond the scope of the present paper, but we are now testing the model sensitivities to assumptions such as partitioning of spring snowmelt, the diurnal cycle, runoff, potential evaporation, and other factors, and are confident that improved models can be developed using the Russian data.

Acknowledgments. We thank Piers Sellers, Yogesh Sud, and Chris Milly for valuable discussions; Robert Dickinson and Cynthia Rosenzweig for valuable reviews; the Main Geophysical Observatory in St. Petersburg for actinometric data; World Data Center B in Obninsk for meteorological data; Bob Etkins, Executive Secretary of Working Group VIII of the US–USSR Agreement on Protection of the Environment, for his support; and Brian Doty for development and enhancements of the GrADS plotting software, which was used for all the figures except Fig. 4. This work is funded by NOAA Grant NA90AA-D-AC804 and NASA Grant NAGW-1269. The views expressed herein are those of the authors and do not necessarily reflect the views of NOAA or any of its subagencies.

REFERENCES

Abramopoulos, F., C. Rosenzweig, and B. Choudhury, 1988: Improved ground hydrology calculations for global climate models (GCMs): Soil water movement and evapotranspiration. *J. Climate,* **1,** 921–941.

Budyko, M. I., 1956: *Heat Balance of the Earth's Surface* (in Russian). Gidrometeoizdat, 255 pp.

Delworth, T., and S. Manabe, 1988: The influence of potential evaporation on the variabilities of simulated soil wetness and climate. *J. Climate,* **1,** 523–547.

——, and ——, 1989: The influence of soil wetness on near-surface atmospheric variability. *J. Climate,* **2,** 1447–1462.

Dickinson, R. E., A. Henderson-Sellers, P. J. Kennedy, and M. F. Wilson, 1986: Biosphere–Atmosphere Transfer Scheme (BATS) for the NCAR Community Climate Model. NCAR Tech. Note TN-275+STR, National Center for Atmospheric Research, Boulder, CO, 69 pp.

Dooge, J. C. I., 1992: Sensitivity of runoff to climate change: A Hortonian approach. *Bull. Amer. Meteor. Soc.,* **73,** 2013–2024.

Dorman, J. L., and P. J. Sellers, 1989: A global climatology of albedo, roughness length, and stomatal resistance for atmospheric general circulation models as represented by the simple biosphere model (SiB). *J. Appl. Meteor.,* **28,** 833–855.

Gandin, L. S., 1965: *Objective Analysis of Meteorological Fields.* Gidrometeoizdat, 242 pp.

Gleick, P. H., 1989: Climate change, hydrology, and water resources. *Rev. Geophys.,* **27,** 329–344.

Hahn, C. J., S. G. Warren, J. London, R. M. Chervin, and R. Jenne, 1984: Atlas of simultaneous occurrence of different cloud types over land. NCAR Tech. Note NCAR/TN-241+STR, National Center for Atmospheric Research, Boulder, CO, 21 pp. + 188 maps.

Hansen, J., G. Russell, D. Rind, P. Stone, A. Lacis, S. Lebedeff, R. Ruedy, and L. Travis, 1983: Efficient three-dimensional global models for climate studies: Models I and II. *Mon. Wea. Rev.*, **111**, 609–662.

Henderson-Sellers, A., A. J. Pitman, and R. E. Dickinson, 1990: Sensitivity of the surface hydrology to the complexity of the land-surface parameterization scheme employed. *Atmosfera*, **3**, 183–201.

——, Z.-L. Yang, and R. E. Dickinson, 1993: The project for intercomparison of land-surface parameterization schemes (PILPS). *Bull. Amer. Meteor. Soc.*, **74**, 1335–1349.

Justice, C. O., J. R. G. Townshend, B. N. Holben, and C. J. Tucker, 1985: Analysis of the phenology of global vegetation using meteorological satellite data. *Int. J. Remote Sens.*, **6**, 1271–1318.

Manabe, S., 1969: Climate and the ocean circulation. 1: The atmospheric circulation and the hydrology of the earth's surface. *Mon. Wea. Rev.*, **97**, 739–774.

——, R. T. Wetherald, and R. J. Stouffer, 1981: Summer dryness due to an increase of atmospheric CO_2-concentration. *Clim. Change*, **3**, 347–386.

Miller, J. R., and G. L. Russell, 1992: The impact of global warming on river runoff. *J. Geophys. Res.*, **97**, 2757–2764.

Milly, P. C. D., 1992: Potential evaporation and soil moisture in general circulation models. *J. Climate*, **5**, 209–226.

Mintz, Y., and Y. V. Serafini, 1992: A global monthly climatology of soil moisture and water balance. *Climate Dyn.*, **8**, 13–27.

Mitchell, J. F. B., 1983: The hydrological cycle as simulated by an atmospheric general circulation model. *Variations in the Global Water Budget*, A. Street-Perrott, M. Beran, and R. Ratcliffe, Eds., Reidel, 429–446.

Monteith, J. L., 1961: An empirical method for estimating longwave radiation exchanges in the British Isles. *Quart. J. Roy. Meteor. Soc.*, **87**, 171–179.

Nobre, C. A., P. J. Sellers, and J. Shukla, 1991: Amazonian deforestation and regional climate change. *J. Climate*, **4**, 957–988.

Palmer, W. C., 1968: Keeping track of crop moisture conditions nationwide: The new crop moisture index. *Weatherwise*, **21**, 156–161.

Sato, N., P. J. Sellers, D. A. Randall, E. K. Schneider, J. Shukla, J. L. Kinter III, Y.-T. Hou, and E. Albertazzi, 1989: Effects of implementing the simple biosphere model in a general circulation model. *J. Atmos. Sci.*, **46**, 2757–2782.

Satterlund, D. R., 1979: An improved equation for estimating longwave radiation from the atmosphere. *Water Resour. Res.*, **15**, 1649–1650.

Schemm, J., S. Schubert, J. Terry, and S. Bloom, 1992: Estimates of monthly mean soil moisture for 1979–1989. NASA Tech. Memo. 104571, National Aeronautics and Space Administration, Greenbelt, MD, 260 pp.

Sellers, P. J., and J. L. Dorman, 1987: Testing the simple biosphere model (SiB) using point micrometeorological and biophysical data. *J. Climate Appl. Meteor.*, **26**, 622–651.

——, Y. Mintz, Y. C. Sud, and A. Dalcher, 1986: A simple biosphere model (SiB) for use within general circulation models. *J. Atmos. Sci.*, **43**, 505–531.

——, W. J. Shuttleworth, J. L. Dorman, A. Dalcher, and J. M. Roberts, 1989: Calibrating the simple biosphere model for Amazonian tropical forest using field and remote sensing data. Part I: Average calibration with field data. *J. Appl. Meteor.*, **28**, 727–759.

Shukla, J., C. Nobre, and P. Sellers, 1990: Amazon deforestation and climate change. *Science*, **247**, 1322–1325.

Vinnikov, K. Y., and I. B. Yeserkepova, 1991: Soil moisture: Empirical data and model results. *J. Climate*, **4**, 66–79.

Williamson, D. L., J. T. Kiehl, V. Ramanathan, R. E. Dickinson, and J. J. Hack, 1987: Description of NCAR Community Climate Model (CCM1). NCAR Tech. Note TN-285+STR, National Center for Atmospheric Research, Boulder, CO, 112 pp.

Wilson, C. A., and J. F. B. Mitchell, 1987: A doubled CO_2 climate sensitivity experiment with a global climate model including a simple ocean. *J. Geophys. Res.*, **92**, 13 315–13 344.

Xue, Y., P. J. Sellers, J. L. Kinter, and J. Shukla, 1991: A simplified biosphere model for global climate studies. *J. Climate*, **4**, 345–364.